Digital Beamforming Synthetic Aperture Radar

Developments at NASA/Goddard Space Flight Center

Rafael Rincon, Temilola Fatoyinbo, Batuhan Osmanoglu, Seung Kuk Lee, Cornelis F. du Toit, Martin Perrine, K. Jon Ranson, Guoqing Sun, Manohar Deshpande, Jaclyn Beck, Daniel Lu, and Tobias Bollian

NASA Goddard Space Flight Center,
Greenbelt, MD, USA

Abstract— **Advanced Digital Beamforming (DBF) Synthetic Aperture Radar (SAR) technology is an area of research and development pursued at the NASA Goddard Space Flight Center (GSFC). Advanced SAR architectures enhances radar performance and opens a new set of capabilities in radar remote sensing. DBSAR-2 and EcoSAR are two state-of-the-art radar systems recently developed and tested. These new instruments employ multiple input-multiple output (MIMO) architectures characterized by multi-mode operation, software defined waveform generation, digital beamforming, and configurable radar parameters. The instruments have been developed to support several disciplines in Earth and Planetary sciences. This paper describes the radars advanced features and report on the latest SAR processing and calibration efforts.**

Keywords—component; Digital Beamforming, interferometry SAR, InSAR.

INTRODUCTION

Synthetic Aperture Radar (SAR) systems are indispensable tools in the observation of Earth and Planetary physical properties, as well as in the detection and identification of natural and man-made structures and objects. SAR's unique ability to provide high resolution images in two or three dimensions over large areas, day or night, and under different weather conditions makes it very suitable for remote sensing studies. The applications of SAR span a wide range of scientific, commercial, and military areas, which employ polarimetry, and interferometry techniques [1].

Emerging SAR imaging techniques have the potential to enhance SAR sensor performance and open a new set of capabilities for future SAR systems. On the forefront of this technological advancement is digital beamforming on receive (thereafter DBF). DBF systems expand the capabilities of remote sensing radars by enabling new measurements and techniques, which overcome several inherent limitations in conventional radar designs [2]. DBSAR-1, an airborne L-band SAR instrument developed at the NASA/Goddard Space Flight Center (GSFC) as a test-bed for DBF, demonstrated the operation, calibration, benefits and capabilities of a multi-mode DBF instrument [2][3] (see Fig. 1).

Moreover, recent advances in radar, electronics, and digital processing technologies have made a new class of radar systems that further enhance SAR sensor performance possible. These new Next Generation Digital Beamforming Synthetic Aperture Radar systems incorporate advanced features including Multiple Input Multiple Output (MIMO) [4][5][6], smart radar waveforms, waveform diversity [5], wideband operation, and full polarimetry. NASA/GSFC's recent developments of EcoSAR [7][8] and DBSAR-2 [9][10] are two such systems. These Next Generation DBF SAR
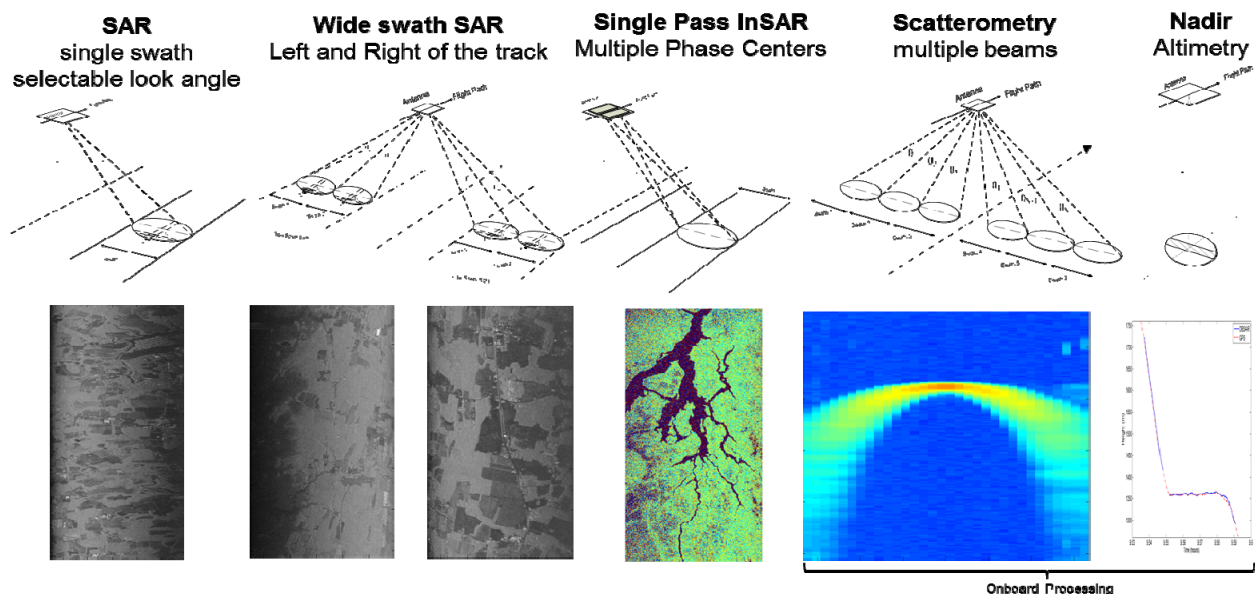

Fig. 1. DBF techniques demonstrated with NASA's DBSAR-1 instrument.

instruments were designed to provide high quality data in support of several disciplines in Earth and planetary sciences, and to set a path for future spaceborne and airborne SAR missions.

The P-band (435 MHz) EcoSAR and L-band (1.26 GHz) DBSAR-2 system architectures build upon the technology path set out by the L-band DBSAR-1 [2], and incorporate recent state-of-the-art technologies developed under NASA Earth Science Technology Office (ESTO) programs and Small Business Innovation and Research (SBIR) investments. New features include multi-channel digital arbitrary waveform synthesis and processing, high resolution DBF, multiple incidence angle, and full polarimetry.

The EcoSAR and DBSAR-2 measurements are applicable to a number of science study areas ranging from ecosystem structure, surface and sub-surface topography, soil freeze-thaw, ice sheet composition, glacier depth, and surface water, among many others. In particular, their measurements can provide unique information on vegetation volumes and densities that can be used to map aboveground biomass, forest cover, disturbance from deforestation and degradation, forest recovery, and wetland inundation, helping us quantify carbon release into the atmosphere [7]. The measurements can also provide an efficient way to detect and document the surface expression of thawing permafrost, helping us quantify the spatial extent of thawing and the accelerating rate of CO_2 and CH_4 gas fluxes to the atmosphere, helping us improve our understanding of the carbon cycle [11].

Furthermore, the large bandwidth and beamforming operation in these instruments expands their scientific measuring capability by permitting the co-incident reception and processing of reflected signals of opportunity (SoOp) [12]. This capability enables the retrieval of complementary geophysical data, including ocean surface roughness (winds), sea surface height, soil moisture, and ice classification, all relevant to climate change studies.

RADAR ARCHITECTURE

EcoSAR and DBSAR-2 employ state-of-the-art radar architectures that perform cross-track scanning using software defined beam steering on transmit (no phase-shifters or moving parts) and digital beamforming on receive. The instruments architectures are characterized by multiple transmit/receive channels (T/R) with software defined waveform generation for each radar transmit channel and dedicated digital receivers for each radar receive channel.

In each of the radars, a set of 8 radar T/R channels (see Fig. 2) operates a fixed polarization (horizontal or vertical). In order to generate a transmit beam with particular beam characteristics and look angle at a given polarization, the radar generates 8 independent waveforms with predefined amplitude and phase at each of the 8 radar channels. On receive, beams are digitally beamformed at each polarization with the desired beam characteristics and look angle. Performance parameters and characteristics achieved with this architecture are listed on Table 1.

Center Frequency	435 MHz (P-band)	1.26 GHz (L-band)
Bandwidth	200 MHz	50 MHZ *, 200 MHz
PRF	1 KHz to 10 kHz	1 KHz to 10 kHz
Pulse Width	10µs to 30 µs	10µs to 30 µs
Number of Channels	32	16
Polarization	HH, VV, VH, HV	H_RH_R, V_RV_R, V_RH_R, H_RV_R H_RH_L, V_RV_L, V_RH_L, H_RV_L H_LH_R, V_LV_R, V_LH_R, H_LV_R H_LH_L, V_LV_L, V_LH_L H_LV_L *
Range Resolution	0.75 m	3 m
Max. Radiated Power	40 W per polarization	16 W per polarization
Beam Steering Range	± 45 degrees	± 45 degrees
Antenna Type	Stack-Patch Array	Stack-Patch Array
Antenna Size	2.9 m x 0.8 m	1 m x 1 m
Number of Subarrays	10	10
Elements per subarray	8	2

* Right (R) side and left (L) side antenna

Both instrument architectures comprise three main subsystems: the antenna array, the Radar Electronics Unit (REU), and the Radar Digital Unit (RDU), as illustrated in Fig. 2 where a set of 8 channels is shown (one polarization only).
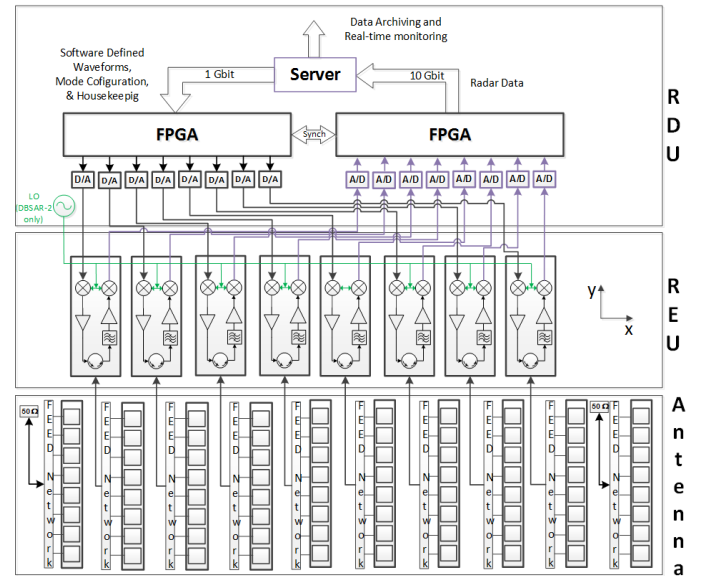

Fig. 2. EcoSAR and DBSAR-2 are based on multi-channel architectures, software defined waveform generation for each transmit channel, dedicated digital receivers for each receive channel, on board processing.

Antenna:

The instruments employ array antennas in a nadir looking orientation, as illustrated in the NASA P-3 aircraft configuration of Fig. 3. EcoSAR uses two P-band antennas mounted under the wings of the aircraft. The centers of the

antennas are separated by a distance (or baseline) of 25 m for interferometric operation. The antennas are 2.9 m in length (cross-track dimension) and 0.8 m in width (along-track dimension). DBSAR-2 uses a one L-band array antenna mounted in the instrument bay in the lower part of the fuselage. The antenna has dimensions of 1 m x 1 m.
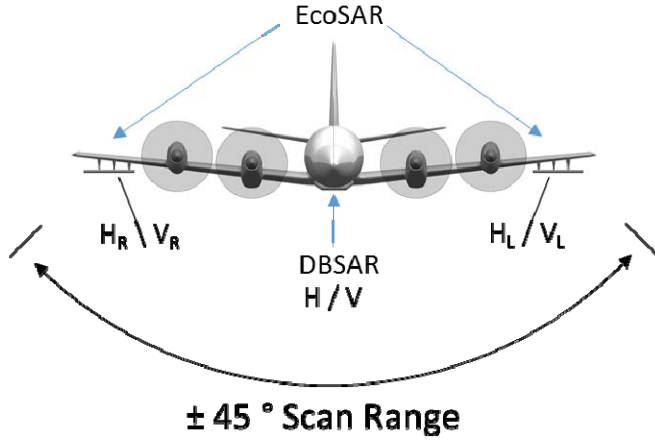

Fig. 3. Illustration of EcoSAR's two wing mounted antennas and DBSAR-2 fuselage mount antenna in a P3 aircraft configuration. The linearly polarized antennas (H and V pol) are nadir pointing permitting a beam steering over a range of ± 45 degrees.

The antenna designs are based on custom stacked-patch elements (see Fig. 4) that permit horizontal (H) and vertical (V) polarimetric radar measurements over large bandwidths (200 MHz in EcoSAR and up to 500 MHz in DBSAR-2) and cross-polarization isolation greater than 30 dB. The antenna elements are grouped as subarrays aligned in the flight direction that permit cross-track beam steering over a range of ± 45 degrees.
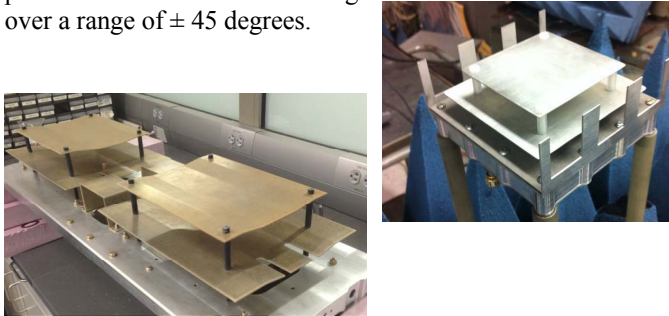

Fig. 4. EcoSAR (left) and DBSAR-2 stacked-patch antenna elements are custom designs to meet the scanning, bandwidth, and cross-polarization requirements of many science applications.

The full size array antenna configuration groups the antenna elements into 10 subarrays (10 x 2 in EcoSAR and 10 x 8 in DBSAR-2). The inner 8 subarrays are active while the first and last subarrays are terminated into 50 ohms to minimize the uneven coupling in the scanning plane, as illustrated in Fig. 2. The EcoSAR antennas are enclosed in an aerodynamic fairing designed and built by the Department of Aerospace Engineering at the University of Kansas [13], as shown in Fig. 5 (left). The DBSAR-2 antenna (Fig. 5 right) employs a flat radome for operation in the instrument bay

under the fuselage of the NASA P3 aircraft. An aerodynamic fairing has also been designed and fabricated for external installation on the NASA C-130 aircraft.

Fig. 5. EcoSAR (left) and DBSAR-2 (right) antennas.

The Radar Electronics Units (REU):

The REU consists of a reference clock generation and distribution stage, and multiple T/R modules. The modules, shown in Fig. 6, conditioned the transmit and receive signals, and include closed loops for robust calibration, dynamic beam control and adaptive waveform generation. The modules' transmit path account for dynamic range, impedance matching and signal levels. The receive path was designed in a similar fashion but noise figure and out-of-band rejection had to be considered.
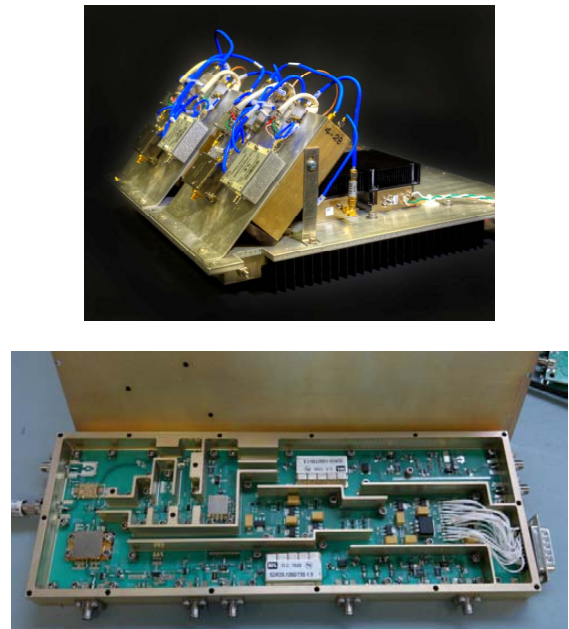

Fig. 6. EcoSAR (top) and DBSAR-2 (bottom) transceiver modules support full polarization operation and provide loopback calibration as well as independent transmit and receive calibrations schemes required for MIMO SAR operation.

EcoSAR operates with 32 T/R modules (8 per polarization). The modules are designed using a hybrid approach where connectorized components are used in the higher power sections of the module and surface-mount on printed circuit board in the other sections (see Fig. 6 top). The modules and power supplies are installed on aircraft racks, which reside inside the aircraft fuselage. Each T/R module outputs a maximum 20-Watt RF power.

DBSAR-2 operates with 16 T/R modules. The modules (see Fig. 6 bottom) were designed on printed circuit boards and used surface mount miniature components to reduce size and volume (dimensions 2.54 cm x 10 cm x 27.6 cm.) while exhibiting high RF performance. Each T/R module outputs a maximum 2-Watt RF power.

The Radar Digital Units (RDUs):

EcoSAR and DBSAR-2 employ custom RDUs capable of multi-channel arbitrary waveform generation, data acquisition, and onboard processing (see fig. 8). The RDUs feature FPGA-based programmable digital waveform generation with multiple time-synchronous and phase-locked digital waveform synthesizers (with independent amplitude and phase control), and a reconfigurable data acquisition and real-time processor with multiple independent receive channels. Each RDU supports 8 radar channels. Figure 7 shows a simplified REU block diagram.

The RDUs, are equipped with Virtex 6 FPGAs, digital-to-analog converters (D/As), and analog-to-digital converters (A/Ds), synthesize based band signals with the appropriate phase and amplitude weights for transmit beam steering and side lobe control. Beamforming on receive can be performed on-board, or processed off-line by coherently capturing the raw complex data. The RDUs are also responsible for radar timing, data transfers, real-time configuration and housekeeping of the instruments, as well as data monitoring and archiving.
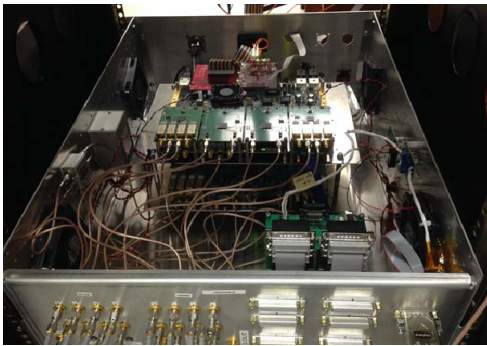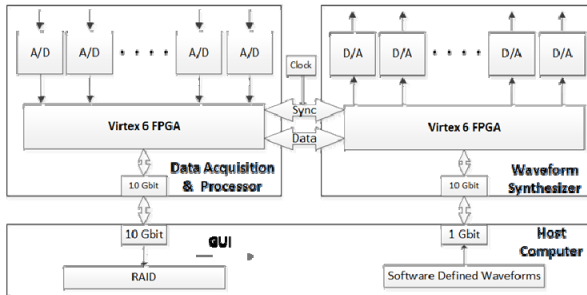

Fig. 7. Multi-channel processor system used by DBSAR-2 and EcoSAR.

The advanced architectures in this radars allow for independent amplitude and phase control at each subarray on transmit, and amplitude and phase measurements between any pair of subarrays on receive, thus enabling across-track scanning. The architecture allows considerable measurement

flexibility including the generation of customized transmit and receive beams, imaging both sides of the flight track (simultaneously or time interleaved), post processing synthesis of multiple beams, variable incidence angle, swath width and ground resolution.

INSTRUMENTS STATUS

Both instruments were extensively tested in the laboratory and calibrated in anechoic chambers. These efforts validate the instruments performance.

The calibration consisted in the characterization of all the radar channels in transmit and receive mode as a function of frequency, the generation of the steering weights, and the measurements of the transmit and receive co-polarized (co-pol) and cross-polarized (cross-pol) patterns.

Figure 8 shows EcoSAR and DBSAR-2 chamber measurements of the one-way "active" transmit patterns for the horizontal polarization at 435 MHz. Four across-track beams are shown corresponding to single sub-array (blue trace), full array - no amplitude taper - steered to boresight (green trace), full array - cosine amplitude taper - steered to boresight (red trace), and cross polarization (magenta trace). Patterns for the vertical polarization were similar to the ones obtained for the horizontal polarization. All patterns, except for DBSAR-2's cross-pol (which is attributed to unwanted chamber reflections), agreed well with theoretical and simulated patterns.
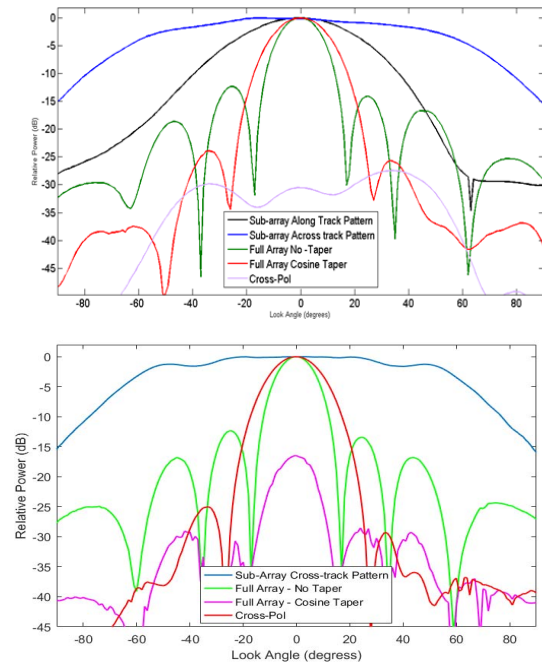

Fig. 8. EcoSAR (top) and DBSAR-2 (bottom) measured active transmit patterns.

EcoSAR flew its first flight campaign in 2014 while DBSAR-2 was just recently completed and will likely fly test in 2017. EcoSAR's first flights were conducted over areas of Andros Island in the Bahamas, and the La Selva and

Corcovado National Parks in Costa Rica in the spring 2014. The instrument flew onboard a NOAA P3 aircraft for approximately 19 hours for data collections and transit to the sites. Field measurements over these areas were also conducted during the same month.

During the campaign, EcoSAR operated in several experimental modes and collected full pol interferometric SAR data at 50 MHz, 120 MHz, and 200 MHz bandwidths in standard and ping pong interferometric modes [14]. Using wide beam illumination mode [2], EcoSAR images swaths on both sides of the flight track without degrading resolution. An example of this simultaneous left-side and right-side imaging over the Corcovado Lake is shown in Fig. 9. The images were acquired at ± 35º look angles from a 3.6 km altitude and multi-looked and re-sampled to yield 5 m x 5 m pixel resolution.
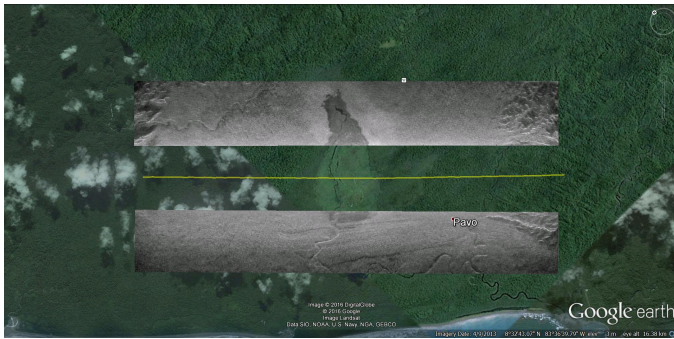

Fig. 9. Horizontal polarization images (H_LH_L) acquired using EcoSAR's simultaneous left-side and right-side of the track imaging over the Corcovado Lake.

EcoSAR's rich data set provides unique information on surface properties of scientific utility. Fig. 10 shows 120 MHz cross-pol Images H_LV_R and H_RV_R, and V_RH_L, and 200 MHz co-pol image V_RV_R, ccorresponding to upper area of Fig. 9. The images show forested areas on the flatlands on the northwest (upper side of image), including the Corcovado Lake and mountains on the southeast (lower side of image).

Fig. 10 shows an RGB image using the Pauli decomposition of EcoSAR's Polarimetric data. Here the red component is obtained from HH-VV, which indicates double single bounce; green is 2×HV, indicating volume scattering from the denser forest; and blue is HH+VV, indicating surface scattering. The results are in good agreement with the physical characteristics of the Corcovado lake area.

The DBSAR-2 instrument development has been now successfully completed and, except for minor firmware upgrades, the system is ready for flight. Because of compactness and size, DBSAR-2 is compatible with a variety of aircrafts. Currently the instrument is configured to fly on NASA's P3 and C-130 aircraft. Configuration on smaller aircraft (e.g., Twin Otter and King Air) is under study.
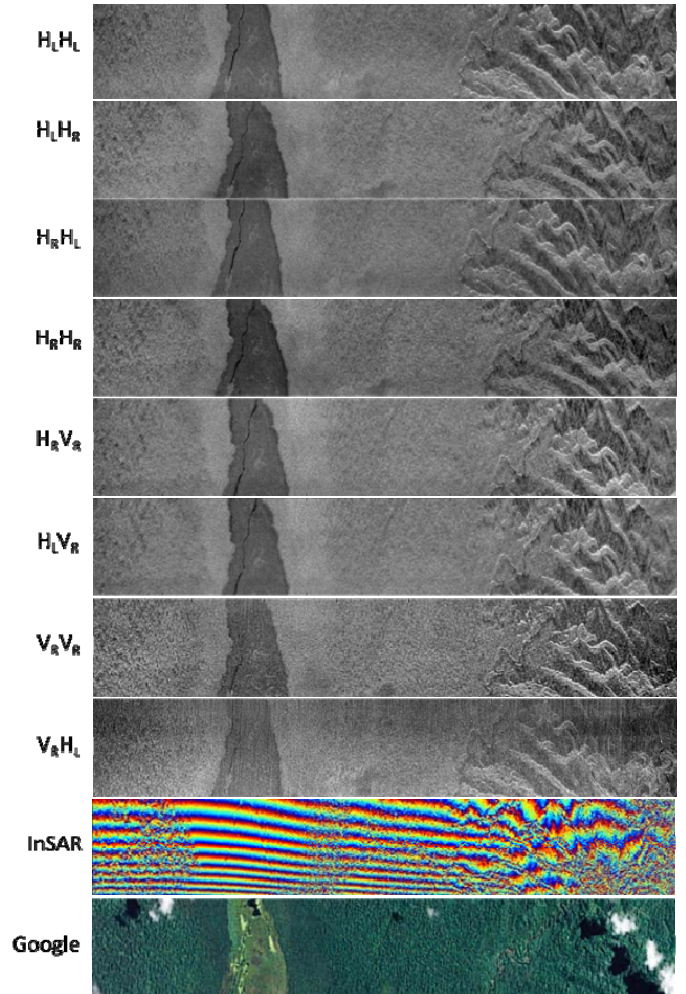

Fig. 10. EcoSAR's 120 MHz co-pol H_LH_L, H_LH_R, H_RH_L, H_RH_R images and cross-pol images H_RV_R , $H_LV_R,$ and V_RH_L, and 200 MHz image V_RV_R.
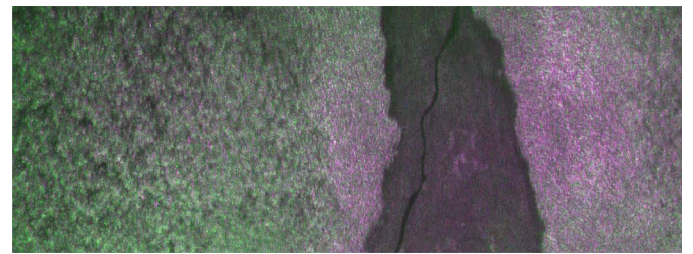

Fig. 11. Pauli decomposition of EcoSAR's Polarimetric data.

Conclusion

Next Generation SAR architectures and imaging techniques promise to enhance SAR sensor performance and open a new set of capabilities for future SAR systems. EcoSAR and DBSAR-2 will help established the Next Generation DBSAR capability as a science instrument while setting a path future Earth science and planetary exploration SAR missions. These systems will be used as test bed for the development and advancement of new imaging techniques.

Flight tests for both instruments are currently being coordinated and a science campaigns will likely take place in 2017.

REFERENCES

[1] Henderson, F. M.; Lewis, A. J. Manual of Remote Sensing, Volume 2: Principles and Applications of Imaging Radar. John Wiley & Sons, New York, 3rd edition, 1998.

[2] Rincon, R. F.; Vega, M. A.; Buenfil, M.; Geist, A.; Hilliard, L.; Racette, P.; 2011A, "NASA's L-Band Digital Beamforming Synthetic Aperture Radar," IEEE Trans. Geosci. Remote Sens.,, vol.49, no.10, pp.3622-3628, Oct. 2011 doi: 10.1109/TGRS.2011.2157971.

[3] Rincon, R.; Fatoyinbo, T.; SeungKuk Lee; Osmanoglu, B.; Ranson, J.; Guoqing Sun; "Digital beamforming synthetic aperture radar (DBSAR): Single-pass interferometry for forest structure estimation". Geoscience and Remote Sensing Symposium (IGARSS), 2015.

[4] Krieger, G; "MIMO-SAR: Opportunities and Pitfalls", IEEE Trans. Geosci. Remote Sens., vol.52, no.5, pp.2628-2645, Jun. 2013.

[5] Krieger, G; Gerbert, N.; and Moreira, A.; "Multidimensional Waveform Encoding: A New Digital Beamforming Technique for Synthetic Aperture Radar Remote Sensing", IEEE Trans. Geosci. Remote Sens.,, vol.46, no.1, pp.31-36, Jan. 2008.

[6] W.-Q. Wang, "Space-time coding MIMO-OFDM SAR for high-resolution imaging," IEEE Trans. Geosci. Remote Sens., vol. 49, no. 8, pp. 3094–3104, Aug. 2011.

[7] Fatoyinbo T., R. Rincon, G. Sun, K. J. Ranson, 2011, EcoSAR: A P-band Digital Beamforming Polarimetric Interferemetric SAR Instrument to Measure Ecosystem Structure and Biomass, Proc. IEEE Int. Geosci. Rem. Sens. Symp., July 25-29, 2011, Vancouver, Canada.

[8] Rincon R., Fatoyinbo T., Ranson K., Osmanoglu B., Lee S., Ranson K. J., Sun G, Perrine M., and Du Toit C.; EcoSAR: P-Band Digital Beamforming Polarimetric And Single Pass Interferometric SAR. Radar Conference, 2015 IEEE. Radar Conference, 2015 IEEE; May 2015.

[9] Rincon, R.; Fatoyinbo, T.; SeungKuk Lee; Osmanoglu, B.; Ranson, J.; Guoqing Sun; Development of NASA's Next Generation L-Band Synthetic Aperture Radar (DBSAR-2). European Synthetic Aperture Radar Conference, June 2016.

[10] Rincon, R.; Fatoyinbo, T.; Osmanoglu, B.; Seung-Kuk Lee; Ranson, K.J.; Marrero, V.; Yeary, M; "Next generation Digital Beamforming Synthetic Aperture Radar (DBSAR-2)". Geoscience and Remote Sensing Symposium (IGARSS), 2015.

[11] Kaab, Andreas; "Remote sensing of permafrost-related problems and hazards"; Permafrost and Periglacial Processes, Volume 19, Issue 2, pages 107–136, April/June 2008.

[12] Shah, R.; Garrison, J.L.; and Grant, M.S., "Demonstration of Bi-static Radar for Ocean Remote Sensing Using Communication Satellite Signals", IEEE Geoscience and Remote Sensing Letters, vol. 9 , no. 4, May 2012.

[13] Hale, R.; Roberts, N., Liu, W., Yang, M., Schroer, D.; Kaushhik, B.; "Flight Safety Review: ECoSAR Integration on the NASA P-3". NASA internal document, June 2013.

[14] P. A. Rosen, S. Hensley, I. R. Joughin, F. K. Li, S. N. Madsen, E. Rodríguez, and R. M. Goldstein, "Synthetic aperture radar interferometry," Proc. IEEE, vol. 88, no. 3, pp. 333–382, Mar. 2000.